3-D description of dip moveout of PS-waves and application to parameter estimation in VTI media

Ilya Tsvankin and Vladimir Grechka
Center for Wave Phenomena, Department of Geophysics, Colorado School of Mines, Golden, CO 80401-1887.

ABSTRACT

Common-midpoint moveout of converted waves is generally asymmetric with respect to zero offset and cannot be described by the traveltime series $t^2(x^2)$ conventionally used for pure modes. Here, we present a concise parametric description of both common-midpoint (CMP) and common-conversion-point (CCP) gathers of PS-waves for arbitrary anisotropic, horizontally layered media above a plane dipping reflector. This analytic representation can be used to generate 3-D (multiazimuthal) CMP gathers without time-consuming two-point ray tracing and obtain such attributes of PS moveout as the slope of the traveltime surface at zero offset and the coordinates of the moveout minimum.

In addition to providing an efficient tool for forward modeling, our formalism helps to carry out joint inversion of P and PS data for transversely isotropic media with a vertical symmetry axis (VTI). If the medium above the reflector is laterally homogeneous, P-wave reflection moveout cannot constrain the depth scale of the model needed for depth migration. Extending our previous results for a single VTI layer, we show that the interval vertical velocities of the P- and S-waves (V_{P0} and V_{S0}) and Thomsen parameters ϵ and δ can be found from surface data alone by combining P-wave moveout with the traveltimes of the converted $PS(PSV)$-wave.

If the data are acquired only on the dip line (i.e., in 2-D), stable parameter estimation requires including the moveout of P- and PS-waves from both a horizontal and a dipping interface. At the first stage of the velocity-analysis procedure, we build an initial anisotropic model by applying a layer-stripping algorithm to CMP moveout of P- and PS-waves. To overcome the distorting influence of reflection-point dispersal on CMP gathers, the obtained interval VTI parameters are refined by resorting the PS data into common-conversion-point (CCP) gathers and repeating the inversion.

For 3-D surveys with a sufficiently wide range of source-receiver azimuths, it is possible to estimate all four relevant parameters (V_{P0}, V_{S0}, ϵ and δ) using moveout from a *single* mildly dipping reflector. In this case, the P-wave NMO ellipse determined by 3-D (azimuthal) velocity analysis is combined with azimuthally dependent traveltimes of the PS-wave. On the whole, the joint inversion of P- and PS data yields a VTI model suitable for both P-wave depth migration and processing (e.g., transformation to zero offset) of converted waves.

Introduction

With recent advances in the acquisition of multicomponent data, such as the technology of ocean bottom surveys, converted waves find an increasing number of applications in seismic exploration. For example, PS-waves help in imaging hydrocarbon reservoirs beneath gas clouds, where conventional P-wave methods fail due to the high attenuation of compressional energy (Thomsen, 1999). Also, converted waves provide information about shear-wave velocities and other medium parameters which cannot be constrained using P-wave data alone. This advantage of mode conversions becomes especially important in anisotropic media due to the multiparameter nature of the inverse problem and the ambiguity in estimating reflector depth from surface P-wave data.

For the transversely isotropic model with a vertical symmetry axis (VTI medium), P-wave reflection traveltimes alone are generally insufficient to determine reflector depth (or vertical velocity) and establish the depth scale of the model. In general, P-wave kinematic signatures in VTI media depend on the vertical velocity V_{P0} and Thomsen's (1986) anisotropic coefficients ϵ and δ (Tsvankin, 1996). However, P-wave moveout in horizontally layered VTI media above a dipping reflector is fully controlled just by the interval normal-moveout (NMO) velocity from a horizontal interface [$V_{\mathrm{nmo},P}(0)$] and the "anellipticity" parameter η (Alkhalifah and Tsvankin, 1995):

$$V_{\mathrm{nmo},P}(0) = V_{P0}\sqrt{1+2\delta}\,, \tag{1}$$

$$\eta = \frac{\epsilon-\delta}{1+2\delta}\,. \tag{2}$$

The parameters $V_{\mathrm{nmo},P}(0)$ and η can be found from the dip dependence of the P-wave NMO velocity or nonhyperbolic (long-spread) moveout of horizontal events and used for all time-domain P-wave processing steps including NMO and dip-moveout (DMO) corrections and time migration (Alkhalifah and Tsvankin 1995; Grechka and Tsvankin 1998a,b). While this time-processing methodology has proved to be quite effective on field data (Alkhalifah et al., 1996; Anderson et al., 1996), the inherent trade-offs between V_{P0}, ϵ and δ in equations (1) and (2) precludes anisotropic parameter estimation in *depth*.

To construct anisotropic models for depth imaging, P-wave reflection traveltimes have to be combined with borehole information (e.g., check shots or well logs), shear or converted waves. In the exploration context, the most practical option is the joint inversion of P- and PS-reflections, particularly for offshore surveys with data collection on the ocean bottom (OBS). Tsvankin and Grechka (1999; hereafter referred to as Paper I) examined this inverse problem in 2-D (i.e., in the dip plane of the reflector) for the model of a single VTI layer. Their analysis shows that it is not sufficient to supplement P-wave NMO velocities from horizontal and dipping reflectors (yielding the parameters $V_{\mathrm{nmo},P}(0)$ and η) with the traveltimes of horizontal PSV events (the PSV-wave will be denoted here simply by PS). To achieve stability in estimating the vertical velocities, the inversion procedure has to include *dip moveout* (i.e., reflection traveltimes from a dipping interface) of PS-waves.

If the reflector is dipping, the common-midpoint moveout curve of the PS-wave is asymmetric with respect to zero offset (i.e., the traveltime does not stay the same if the source and receiver are interchanged) and may not have a minimum for relatively steep dips exceeding 40-50°. Paper I introduces an exact parametric representation of PS-wave moveout on CMP gathers in vertical symmetry planes of anisotropic homogeneous media and gives concise expressions for such attributes of the traveltime curve as the slope at zero offset, NMO velocity at the traveltime minimum etc. For VTI media, those attributes of dipping PS events proved to be sufficiently sensitive to the model parameters for the joint inversion of P- and PS traveltimes to give accurate estimates of the P- and S-wave vertical velocities V_{P0} and V_{S0} and the coefficients ϵ and δ. The main limitations of the algorithm developed in Paper I are the simplicity of the model (2-D, single layer) and the reliance on CMP geometry in which converted modes suffer from reflection-point dispersal.

Here, the methodology of Paper I is extended to more realistic, vertically inhomogeneous anisotropic media above a dipping reflector. We develop general 3-D parametric traveltime-offset relationships for PS-waves recorded on areal CMP and common-conversion-point (CCP) gathers and also provide simplified 2-D expressions valid in vertical symmetry planes of the model. Those analytic results are incorporated into 2-D and 3-D inversion algorithms for VTI media capable of estimating all four relevant parameters (V_{P0}, V_{S0}, ϵ and δ) from P and PS data. It is particularly advantageous to use 3-D wide-azimuth surveys because areal gathers of P and PS reflections from a *single* mildly dipping interface are sufficient for reconstructing a VTI depth model. Numerical examples confirm the accuracy and efficiency of our parameter-estimation methodology for typical layered VTI models.

Parametric description of converted-wave moveout

Conventional-spread reflection moveout of pure modes on CMP gathers in both isotropic and anisotropic media is usually close to a hyperbolic curve parameterized by normal-moveout velocity (e.g., Tsvankin and Thomsen, 1994; Grechka and Tsvankin, 1998b). For mode-converted waves, however, CMP moveout is generally asymmetric with respect to zero offset and cannot be fitted to a hyperbola centered at the CMP location. Only in the special case of horizontally layered media with a horizontal symmetry plane the traveltime of converted waves becomes an even function of the source-receiver offset (Grechka, Theophanis, and Tsvankin, 1999).

Here, we give a parametric representation of reflection moveout of converted waves in layered anisotropic media. The model is composed of a stack of horizontal layers above a generally dipping plane interface. The P-to-S (or S-to-P) conversion is assumed to take place only at the bottom of the model (reflector); Thomsen (1999) suggested to call PS-modes of this type "C-waves."

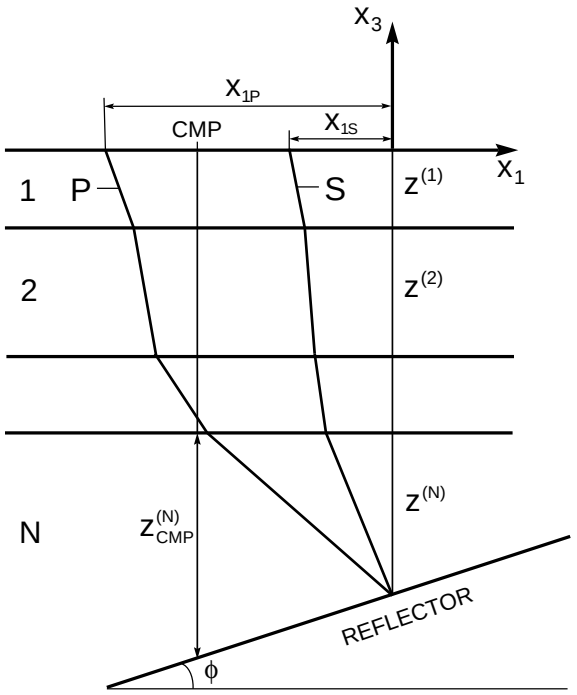

Figure 1. Geometry of the PS-reflection from a dipping interface in a vertical symmetry plane of layered anisotropic media. x_{1P} and x_{1S} are the horizontal coordinates of the (P-wave) source and the receiver; $z^{(\mathrm{N})}$ and $z^{(\mathrm{N})}_{\mathrm{CMP}}$ are the thicknesses of layer N measured above the reflection point and below the common midpoint (CMP), respectively.

First, we treat the 2-D problem of wave propagation in vertical symmetry planes and then proceed with an analytic description of *azimuthally dependent* PS moveout over an arbitrary anisotropic layered model. Exact 2-D and 3-D expressions for the traveltime and offset on both common-conversion-point (CCP) and common-midpoint (CMP) gathers are followed by the derivation and analysis of the moveout attributes needed in the inversion procedure.

2-D expressions for vertical symmetry planes

Suppose the acquisition line is confined to the dip plane of the reflector overlaid by an arbitrary number of horizontal layers (Figure 1). The anisotropic symmetry does not need to be specified at this stage, but the vertical incidence plane is assumed to be a plane of mirror symmetry in all layers. Therefore, both rays and phase-velocity vectors of reflected waves cannot deviate from the dip plane of the reflector, and the kinematics (but not necessarily dynamics) of wave propagation can be treated in two dimensions.

Figure 2 illustrates the behavior of converted-wave moveout on CMP and CCP gathers above a layered VTI medium. Similar to the single-layer case discussed in Paper I, the offset of the traveltime minimum on CMP gathers increases with dip, which makes the moveout curve increasingly asymmetric with respect to $x = 0$. If the dip does not exceed 30-40°, the traveltime minimum can often be recorded on a sufficiently long CMP gather (Figure 2a). For steeper dips the traveltime monotonically decreases with offset (Figure 2c,e), and the short-offset moveout is largely controlled by the slope of the moveout curve at zero offset. The moveout in Figure 2e is truncated because the reflection point at $x \approx 1$ km reaches the intersection of the reflector with the bottom of the second layer (i.e., layer 3 pinches out). This shape of the traveltime function suggests that the moveout attributes of the PS-wave suitable for the parameter-estimation procedure can include the zero-offset moveout slope $dt/dx|_{x=0}$ and, for mild dips, the normalized offset of the traveltime minimum $x_{\min}/t_{\min}$. Another attribute that proved useful in the single-layer model is the NMO velocity of the PS-wave at the traveltime minimum (Paper I), but for stratified VTI media it is difficult to derive it in a closed analytic form.

The dependence of converted-wave CCP moveout on dip is more complicated. For the model in Figure 2, the traveltime minimum first moves towards negative offsets with increasing dip (Figure 2b,d) and then returns back almost to the zero-offset location (Figure 2f).

In principle, the traveltime and offset of the PS-wave on CCP gathers can be found by simply summing up the single-layer 2-D expressions of Paper I. In Appendix A, however, the solution of the 2-D problem, both in CCP and CMP geometry, is found as a special case of the general 3-D equations by aligning the axis x_1 with the dip plane of the reflector and eliminating the projections of the slowness vector on the x_2-axis. The traveltime of the PS arrival with the conversion point an the N-th interface (Figure 1) is given by

$$\begin{aligned} t_{PS} &= t_P + t_S \\ &= \sum_{\ell=1}^{N} z^{(\ell)} \left(q_P^{(\ell)} - p_{1P}\, q_{,1P}^{(\ell)} + q_S^{(\ell)} - p_{1S}\, q_{,1S}^{(\ell)}\right). \end{aligned} \tag{3}$$

where $z^{(\ell)}$ ($\ell = 1, 2, \ldots N-1$) are the thicknesses of the horizontal layers in the overburden, $z^{(\mathrm{N})}$ is the thickness of layer N above the conversion point, $q_P^{(\ell)}$ and $q_S^{(\ell)}$ are the interval vertical slownesses of the P- and S-waves, p_{1P} and p_{1S} are the projections of the slowness vector on the axis x_1 (ray parameters), $q_{,1P}^{(\ell)} \equiv dq_P^{(\ell)}/dp_{1P}$ and $q_{,1S}^{(\ell)} \equiv dq_S^{(\ell)}/dp_{1S}$. Since the medium above the reflector is laterally homogeneous, the ray parameters p_{1P} and p_{1S} remain constant between the reflector and the surface; they are related to each other through Snell's law at the reflector.

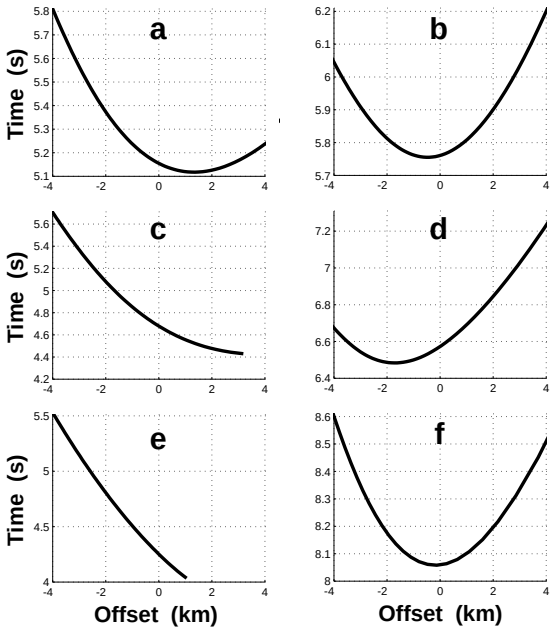

Figure 2. Dip-line moveout of the PS-wave converted at a dipping interface beneath three VTI layers (the top two layers are horizontal). The left column (a,c,e) are common-midpoint (CMP) gathers, the right column (b,d,f) are common-conversion-point (CCP) gathers. Each row corresponds to a different reflector dip ϕ: $\phi = 20^\circ$ (a,b), $\phi = 40^\circ$ (c,d) and $\phi = 60^\circ$ (e,f). For positive offsets the P-wave leg is located downdip from the S-wave leg.
The top layer (layer 1) has the following parameters: $V_{P0}^{(1)} = 2.0$ km/s, $V_{S0}^{(1)} = 0.8$ km/s, $\epsilon^{(1)} = 0.1$, $\delta^{(1)} = 0.05$, the thickness $z^{(1)} = 0.5$ km; for layer 2, $V_{P0}^{(2)} = 2.3$ km/s, $V_{S0}^{(2)} = 1.0$ km/s, $\epsilon^{(2)} = 0.2$, $\delta^{(2)} = 0.1$, $z^{(2)} = 1.5$ km; for layer 3, $V_{P0}^{(3)} = 2.9$ km/s, $V_{S0}^{(3)} = 1.2$ km/s, $\epsilon^{(3)} = 0.15$, $\delta^{(3)} = 0.1$, $z^{(3)} = 2$ km. For CCP gathers, $z^{(3)}$ is the thickness of layer 3 above the common reflection point; for CMP gathers, $z^{(3)}$ is the distance between the projection of the CMP on the top of layer 3 and the reflector.

The source-receiver offset in 2-D geometry is found in Appendix A as

$$x_{PS} = x_{1S} - x_{1P} = \sum_{\ell=1}^{N} z^{(\ell)} \left(q_{,1P}^{(\ell)} - q_{,1S}^{(\ell)}\right). \qquad (4)$$

Since the x_1-axis points updip (Figure 1), the offset x in equation (4) is positive if the P-leg is located *downdip* with respect to the S-leg; the same sign convention was adopted in Paper I.

To compute the traveltime and offset from equations (4) and (4), we need to specify one of the ray parameters (p_{1P} or p_{1S}) and find the other from Snell's law at the reflector. The vertical slownesses $q_P^{(\ell)}$ and $q_S^{(\ell)}$ in each layer, along with the derivatives $q_{,1P}^{(\ell)}$ and $q_{,1S}^{(\ell)}$, can be determined from the Christoffel equation (Grechka, Tsvankin, and Cohen, 1999). Therefore, scanning over one of the ray parameters produces a CCP gather for the conversion point located at the depth $\sum_{\ell=1}^{N} z^{(\ell)}$.

To generate a CMP gather, it is necessary to relate the thickness $z^{(\mathrm{N})}$ of the N-th layer above the CCP to the layer thickness $z_{\mathrm{CMP}}^{(\mathrm{N})}$ beneath the common midpoint (Figure 1). Adapting the corresponding 3-D expression leads to (Appendix A)

$$z^{(\mathrm{N})} = \frac{z_{\mathrm{CMP}}^{(\mathrm{N})} - \frac{\tan\phi}{2} \sum_{\ell=1}^{N-1} \left[z^{(\ell)} \left(q_{,1P}^{(\ell)} + q_{,1S}^{(\ell)}\right)\right]}{1 + \frac{\tan\phi}{2} \left(q_{,1P}^{(\mathrm{N})} + q_{,1S}^{(\mathrm{N})}\right)}. \qquad (5)$$

Substitution of $z^{(\mathrm{N})}$ from equation (5) into equations (4) and (4) yields the traveltime and offset of the PS-wave recorded on the CMP gather specified by $z_{\mathrm{CMP}}^{(\mathrm{N})}$. In the special case of a single layer, the sum over the $N-1$ layers in the numerator has to be dropped, and $z^{(\mathrm{N})}$ reduces to the expression obtained in Paper I.

These analytic expressions make it possible to compute a CMP gather of converted waves in symmetry planes of layered anisotropic media without time-consuming two-point ray tracing. It is still necessary to satisfy Snell's law at the reflector and solve the Christoffel equation in each layer for both P- and S-waves, but the whole computation of t and x for a given source-receiver pair has to be performed only *once* (i.e., for the pair of the ray parameters that corresponds to a single ray). Also, note that in media with a horizontal symmetry plane (e.g., VTI and HTI) the Christoffel equation $q(p) = 0$ has an analytic solution because it reduces to a quadratic polynomial in q^2.

3-D description of PS moveout

Let us consider a PS-wave formed by mode conversion at a plane dipping interface underlying an arbitrary anisotropic homogeneous medium. For recording in CMP geometry, the sources and receivers are placed on lines with different azimuths but the same CMP location (Figure 3). In general, an incident P-wave in such a model excites two reflected shear modes (PS_1 and PS_2) propagating towards the surface with different velocities and polarizations. The formalism introduced below is valid for either PS-wave with the substitution of the appropriate slowness vector.

Using the 3-D relationship between the slowness and group-velocity vectors, the traveltime of the wave reflected (converted) at the depth z_r can be written in the form (Appendix A)

$$\begin{aligned} t_{PS} &= t_P + t_S \\ &= z_r \left(q_P - p_{1P}\, q_{,1P} - p_{2P}\, q_{,2P} \right. \\ &\quad \left. + q_S - p_{1S}\, q_{,1S} - p_{2S}\, q_{,2S}\right), \end{aligned} \qquad (6)$$

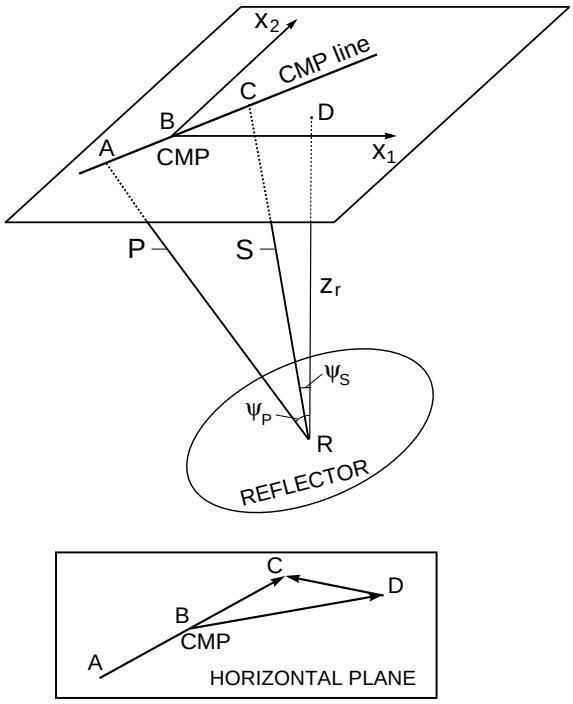

Figure 3. Converted PS-wave (ray ARC) recorded on an arbitrary oriented common-midpoint line over a homogeneous anisotropic layer with a dipping lower boundary. z_r is the depth of the conversion point, ψ_P and ψ_S are the angles between the P- and S-rays and the vertical. The inset shows the source-receiver vector (**AC**), the common midpoint (B) and the projection of the reflection point onto the surface (D).

where the subscript "2" refers to the projections on the x_2-axis, and for each wave $q_{,2} \equiv \partial q/\partial p_2$. As before, the slowness vectors of the P and S-waves are related to each other by Snell's law at the reflector: their projections onto the reflector should be identical.

The source-receiver vector $\mathbf{x}_{PS} = \mathbf{AC}$ (Figure 3) is obtained in Appendix A as

$$\begin{aligned} \mathbf{x}_{PS} &= \{(x_{1S} - x_{1P}),\, (x_{2S} - x_{2P})\} \\ &= z_r\,\{(q_{,1P} - q_{,1S}),\, (q_{,2P} - q_{,2S})\}\,. \end{aligned} \tag{7}$$

Equation (7) yields the following expressions for the source-receiver offset x_{PS} and the azimuth α of the source-receiver line with respect to the x_1-axis:

$$x_{PS} = |\mathbf{x}_{PS}| = z_r\,\sqrt{(q_{,1P} - q_{,1S})^2 + (q_{,2P} - q_{,2S})^2}\,, \tag{8}$$

$$\alpha = \tan^{-1}\left(\frac{q_{,2P} - q_{,2S}}{q_{,1P} - q_{,1S}}\right)\,. \tag{9}$$

Equations (6), (8) and (9) are sufficient for generating common-conversion-point gathers of the PS-wave.

As in the 2-D problem treated in the previous section, common-midpoint moveout can be modeled by replacing z_r with the reflector depth beneath the CMP location [equations (A13) and (A14)]:

$$z_r = \frac{z_{\rm CMP}}{1 + \frac{\tan\phi}{2}\left[(q_{,1P} + q_{,1S})\,\zeta_1 + (q_{,2P} + q_{,2S})\,\zeta_2\right]}\,, \tag{10}$$

where ζ_1 and ζ_2 are the components of a horizontal unit vector that points in the updip direction of the reflector. Equations (6) and (7), with z_r defined in equation (10), produce the traveltime and the source-receiver vector of a PS-wave on the CMP gather described by $z_{\rm CMP}$.

The corresponding expressions for *layered* arbitrary anisotropic media are developed in Appendix A and will not be reproduced here. The parametric 3-D equations for traveltime and offset are particularly convenient for generating the entire areal (3-D) CMP gather, with sources and receivers occupying a wide range of azimuths and offsets. This can be done by scanning over the two horizontal slowness components of one of the waves (e.g., p_{1P} and p_{2P}), obtaining the corresponding slowness vector of the other wave from Snell's law and computing the traveltime and offset from equations (6), (7) and (10) or the more general expressions for layered media (Appendix A). Such an algorithm is orders of magnitude faster than two-point ray tracing for each source-receiver pair in the 3-D CMP gather.

The parametric approach, however, is less efficient in modeling an individual CMP line with a given orientation. In this case, it is necessary to search for the slowness vectors of the P- and S-waves which do not only comply with Snell's law at the reflector, but also satisfy equation (9) for the azimuth of the CMP line. Therefore, it is preferable to compute the whole 3-D gather on a grid of two horizontal slownesses (e.g., of the P-wave) and build needed CMP lines by interpolation from the obtained traveltime table.

Attributes of the moveout curve

Moveout slope at zero offset

Since common-midpoint traveltime of converted waves is generally asymmetric with respect to $x = 0$, short-spread moveout is largely controlled by the slope of the moveout curve at zero offset (rather than by the NMO velocity, as is the case for pure modes). The zero-offset moveout slope of the PS-wave in a VTI layer is quite sensitive to the anisotropic parameters and represents a useful attribute for moveout inversion (Paper I).

Paper I also shows that the slope (apparent slowness) of the CMP moveout curve of any pure or converted wave recorded in a vertical symmetry plane is equal to one-half of the difference between the ray parameters (horizontal slownesses) at the source and receiver locations. A 3-D generalization of this result for CMP traveltime in arbitrary anisotropic heterogeneous media is given in Appendix B:

$$\left.\frac{dt}{dx}\right|_{\mathbf{x}} = \frac{1}{2}\left[p_{\rm R}(h,\,\alpha) - p_{\rm I}(-h,\,\alpha)\right]\,, \tag{11}$$

where $\left.\frac{dt}{dx}\right|_{\mathbf{x}}$ is the reflection slope on a CMP line described by the source-receiver vector $\mathbf{x}$, $h \equiv |\mathbf{x}|/2$ is half the source-receiver offset, and $p_{\rm I}(h,\,\alpha)$ and $p_{\rm R}(h,\,\alpha)$ are the projections of the slowness vectors of the incident and reflected rays on the CMP-line azimuth α; the positive direction of the CMP line is taken from the source to the receiver. In general, $p_{\rm I}(h,\,\alpha)$ and $p_{\rm R}(h,\,\alpha)$ should be evaluated at the source and receiver locations (respectively), but in our model each ray parameter remains constant between the reflector and the surface. Note that $p_{\rm I}(h,\,\alpha)$ and $p_{\rm R}(h,\,\alpha)$ also are the quantities required to build the so-called RTM gathers introduced in a companion paper (Grechka and Tsvankin, 2000).

To obtain the moveout slope at $x = 0$ in the 2-D problem, we need to compute the values of $p_{1P} = p_{\rm I}$ and $p_{1S} = p_{\rm R}$ for the zero-offset PS ray. The source-receiver offset in CMP geometry can be found from equation (4) with $z^{(\rm N)}$ defined in equation (5). Setting the offset x in equation (4) to zero yields an equation that can be solved for one of the ray parameters (e.g., p_{1P}); the other ray parameter is determined from Snell's law at the reflector.

A similar procedure can be devised for the 3-D problem. The slownesses of the P- and S-legs of the zero-offset ray should be obtained by setting x_{PS} [equation (8) for a single layer and (A18) for layered media] for a given $z_{\rm CMP}$ to zero and taking Snell's law into account. Then the slowness vectors are projected onto the CMP line, and the slope of the moveout curve at zero offset is computed from equation (11).

Normalized offset of the traveltime minimum

For relatively mild dips up to 30-40°, the common-midpoint traveltime curve of the PS-wave usually has a minimum ($t_{\rm min}$) at a certain offset $x_{\rm min}$ (Figure 2). The normalized offset $x_{\rm min}/t_{\rm min}$ served as another attribute in the single-layer inversion procedure introduced in Paper I.

For the stratified 2-D model, the values of $x_{\rm min}$ and $t_{\rm min}$ can be found from equations (4), (4) and (5), where the ray parameters $p_{1P} = p_{\rm I}$ and $p_{1S} = p_{\rm R}$ should correspond to the traveltime minimum. Since at $x = x_{\rm min}$ the slope of the moveout curve goes to zero, the ray parameters should be equal to each other: $p_{1P} = p_{1S} = p^{\rm min}$ [see equation (11)]; $p^{\rm min}$ is determined from Snell's law at the reflector. Then the ratio $x_{\rm min}/t_{\rm min}$ is given by

$$\frac{x_{\rm min}}{t_{\rm min}} = \left.\frac{\sum_{\ell=1}^{N} z^{(\ell)}\,(q_{,P}^{(\ell)} - q_{,S}^{(\ell)})}{\sum_{\ell=1}^{N} z^{(\ell)}\,(q_P^{(\ell)} - p^{\rm min} q_{,P}^{(\ell)} + q_S^{(\ell)} - p^{\rm min} q_{,S}^{(\ell)})}\right|_{p^{\rm min}} \quad (12)$$

Note that, in contrast to the single-layer model, the normalized offset $x_{\rm min}/t_{\rm min}$ from equation (12) depends not only on the elastic parameters and reflector dip (Paper I), but also on the layer thicknesses.

Likewise, in the 3-D model the traveltime minimum on a CMP line with a given azimuth α corresponds to equal values of the slowness projections $p_{\rm R}(h,\,\alpha) = p_{\rm I}(-h,\,\alpha) = p^{\rm min}$ which can be found from Snell's law.

Parameter estimation in layered VTI media

The formalism introduced above is valid for PS moveout in horizontally layered, arbitrary anisotropic media above a dipping reflector. Below, these general results are combined with known expressions for the dip-dependent NMO velocity of P-waves to develop a parameter-estimation methodology for transversely isotropic media with a vertical symmetry axis (VTI). We start with an overview of the 2-D inversion algorithm for the single-layer model and proceed with a description of 2-D and 3-D moveout-inversion procedures for stratified VTI media.

Review of the 2-D single-layer algorithm

The goal of the parameter-estimation methodology introduced in Paper I is to invert the moveout of P and PS-waves from both a horizontal and a dipping reflector for the P- and S-wave vertical velocities (V_{P0} and V_{S0}) and the anisotropic coefficients ϵ and δ. P-wave reflection moveout in a VTI layer is fully governed by the parameters $V_{{\rm nmo},P}(0)$ and η [equations (1) and (2)] and, therefore, yields two equations for the medium parameters. The remaining information for the inversion is provided by the moveout of converted modes and the ratios of the zero-offset traveltimes of P- and PS-waves.

The moveout curve of the PS-wave from a horizontal reflector is symmetric with respect to zero offset because the VTI model has a horizontal symmetry plane. Furthermore, typically PS traveltimes on CMP spreads limited by reflector depth can be adequately described by the NMO velocity defined in the same way as that for pure modes (Grechka, Theophanis and Tsvankin, 1999). NMO velocities of pure and converted modes in horizontally layered VTI media are related by the following Dix-type equation (Seriff and Sriram 1991; Tsvankin and Thomsen, 1994):

$$t_{PS0}\,V_{{\rm nmo},PS}^2(0) = t_{P0}\,V_{{\rm nmo},P}^2(0) + t_{S0}\,V_{{\rm nmo},SV}^2(0)\,, \quad (13)$$

where t_{P0} and t_{S0} are the vertical traveltimes of the P and S-waves, and $t_{PS0} = t_{P0} + t_{S0}$. Hence, combining P and PS data allows us to determine the SV-wave NMO velocity $V_{{\rm nmo},SV}(0)$ given (for a single VTI layer) by

$$V_{{\rm nmo},SV}(0) = V_{S0}\sqrt{1+2\sigma}\,, \quad (14)$$

$$\sigma \equiv \left(\frac{V_{P0}}{V_{S0}}\right)^2 (\epsilon - \delta)\,. \quad (15)$$

Therefore, horizontal P and PS events in a VTI

layer can be used to obtain the NMO velocities of P-waves [equation (1)] and SV-waves [equation (15)]. Also, the vertical-velocity ratio $\kappa \equiv V_{P0}/V_{S0}$ can be deduced from the vertical traveltimes of P- and PS-waves. This set of input data provides three constraints on four unknown medium parameters. Hence, for a given value of one of the parameters (e.g., δ), we can determine the other three from the horizontal events (Paper I):

$$V_{P0} = \frac{V_{\mathrm{nmo},P}(0)}{\sqrt{1+2\delta}}\,, \tag{16}$$

$$V_{S0} = \frac{V_{P0}}{\kappa}\,, \tag{17}$$

$$\sigma = \frac{1}{2}\left[\frac{V^2_{\mathrm{nmo},SV}(0)}{V^2_{S0}} - 1\right]\,, \tag{18}$$

$$\epsilon = \frac{\sigma}{\kappa^2} + \delta\,. \tag{19}$$

Next, the moveout of dipping events has to be inverted for the anisotropic coefficient δ. In principle, it seems to be sufficient to obtain the parameter η [equation (2)] using the P-wave NMO velocity from a dipping reflector. In this case, however, the parameter-estimation procedure is too unstable to be used in practice because small errors in $\eta \approx \epsilon - \delta$ propagate with significant amplification into the vertical velocities [Paper I; see equations (14) and (15)]. A significant improvement can be achieved by including the moveout attributes of the PS-wave reflected from the same dipping interface. The attributes used in the single-layer problem are the slope of the moveout curve at zero offset, and, if the PS-wave traveltime has a minimum $t_{\min}(x_{\min})$ on the CMP gather, the normalized offset $x_{\min}/t_{\min}$ and the NMO velocity defined at $x = x_{\min}$. Numerical examples in Paper I confirm the accuracy and stability of this inversion methodology in the presence of realistic errors in input data.

2-D inversion in layered VTI media

Stage 1: CMP gathers

The analytic 2-D expressions for PS moveout given above are valid if the dip plane of the reflector coincides with a vertical symmetry plane of all layers in the overburden. For example, if the medium is orthorhombic with two mutually orthogonal symmetry planes, our formalism can be used for two specific orientations of the reflector confined to the symmetry planes. (For any other reflector orientation, the 2-D equations are applicable only under the assumption of weak azimuthal anisotropy.) For azimuthally isotropic VTI media, however, there are no restrictions on the direction of reflector strike because each vertical plane is a plane of symmetry.

Since resorting into CCP gathers requires knowledge of model parameters, at the first stage of the inversion procedure, the interval values of the parameters V_{P0}, V_{S0}, ϵ and δ are estimated using P and PS data collected into CMP gathers. Suppose the model consists of several horizontal VTI layers intersected by a dipping interface (e.g., by a fault plane, see Figure 4). After having determined the parameters of the subsurface layer using the algorithm described above, we proceed with the moveout inversion for the second layer. The first step is to use horizontal P and PS events to determine the interval NMO velocities of P and $S(SV)$-waves. Combining P- and PS-wave NMO velocities for reflections from the bottom of the second layer, we obtain the corresponding S-wave NMO velocity from equation (13). Then the interval P- and S-wave NMO velocities in the second layer are found using the conventional Dix differentiation (e.g., Tsvankin and Thomsen, 1994, 1995). The ratio of the interval vertical velocities in layer 2 ($\kappa^{(2)} \equiv V^{(2)}_{P0}/V^{(2)}_{S0}$) can be determined in a straightforward way from the zero-offset traveltimes of the P- and PS-waves.

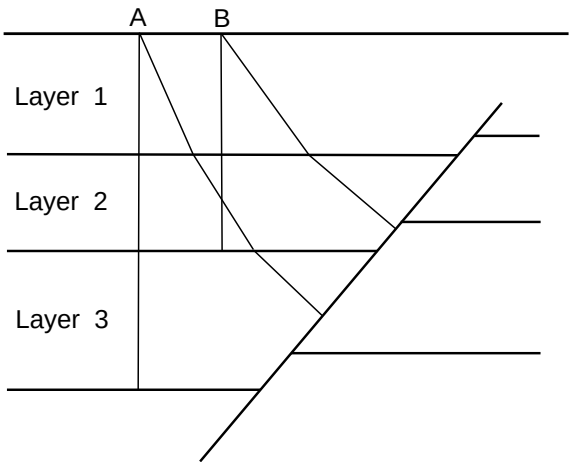

Figure 4. Zero-offset P-wave rays in a layered VTI medium with a throughgoing fault plane. The inversion algorithm operates with reflection moveout from horizontal and dipping interfaces in each depth interval. The dipping events in layers 2 and 3 are recorded at CMP locations B and A, respectively.

Thus, the horizontal events yield the three interval parameters required by the single-layer inversion algorithm ($V^{(2)}_{\mathrm{nmo},P}(0)$, $V^{(2)}_{\mathrm{nmo},SV}(0)$ and $\kappa^{(2)}$). Using these results and equations (16)–(19), we can express the interval parameters of the second layer through the anisotropic coefficient $\delta^{(2)}$ exactly in the same way as in the single-layer problem.

Then dipping P and PS events generated in the second layer can be inverted for $\delta^{(2)}$ and, therefore, for the full set of the interval parameters. The layer-stripping of dipping P-wave events in layered VTI media is described in detail by Alkhalifah and Tsvankin (1995) and Alkhalifah (1997). Their algorithm makes it possible to

find the interval NMO velocity $V^{(2)}_{\mathrm{nmo},P}(p^{(2)}_{P0})$ of the dipping P-wave event in the second layer, where $p^{(2)}_{P0}$ is the ray parameter of the zero-offset P-wave reflection from the dipping interface that can be determined from the reflection slope on the zero-offset section. To obtain $V^{(2)}_{\mathrm{nmo},P}(p^{(2)}_{P0})$ from the effective NMO velocity of the dipping event, it is necessary to know two parameters of the subsurface layer – the zero-dip NMO velocity $V^{(1)}_{\mathrm{nmo},P}(0)$ and the coefficient $\eta^{(1)}$.

As discussed above, the moveout of horizontal events and the NMO velocity $V^{(2)}_{\mathrm{nmo},P}(p^{(2)}_{P0})$ have to be supplemented with the DMO attributes of the converted wave for estimating the medium parameters with sufficient accuracy. Our inversion algorithm operates with two such attributes – the slope of the moveout curve at zero offset ($dt/dx|_{x=0}$) and, for mild dips, the normalized offset of the traveltime minimum. (A more elaborate approach that uses PS traveltimes for a wider range of offsets is briefly outlined below.) To recover the moveout slope at zero offset, we approximate short-spread PS traveltimes with a shifted hyperbola, as discussed in Paper I. The coefficients of the hyperbola are found either by the least-squares method (if the traveltimes have been picked) or by semblance analysis of the seismograms.

Computation of the zero-offset moveout slope and the normalized offset of the traveltime minimum of the PS-wave for a layered VTI model using equations (4), (5) and (11) is described above. To define a "trial" model, we start with a certain value of the anisotropic coefficient $\delta^{(2)}$ and obtain the other parameters of the second layer using horizontal events. The dip of the reflector and the thickness of the second layer beneath the CMP ($z^{(2)}_{\mathrm{CMP}}$) – quantities needed to determine the moveout attributes of the PS-wave – are calculated from the zero-offset traveltime of the dipping P event and the ray parameter $p^{(2)}_{P0}$. Hence, the horizontal events and the P-wave reflection from the dipping interface allow us to completely define the trial model that corresponds to the chosen value of $\delta^{(2)}$.

Finally, $\delta^{(2)}$ (and, consequently, the full parameter set of the second layer) is obtained by minimizing the objective function

$$\mathcal{F}_{\mathrm{CMP}} = \left[\frac{V_{\mathrm{nmo},P}(p_{P0}) - V^{\mathrm{meas}}_{\mathrm{nmo},P}(p_{P0})}{V^{\mathrm{meas}}_{\mathrm{nmo},P}(p_{P0})}\right]^2 + \left[\frac{(dt/dx|_{x=0}) - (dt/dx|_{x=0})^{\mathrm{meas}}}{(dt/dx|_{x=0})^{\mathrm{meas}}}\right]^2 + \left[\frac{(x_{\min}/t_{\min}) - (x_{\min}/t_{\min})^{\mathrm{meas}}}{(x_{\min}/t_{\min})^{\mathrm{meas}}}\right]^2, \quad (20)$$

where the superscript "meas" denotes the measured values, and the quantities without a subscript are computed for a trial VTI model. The function (20) represents a system of three nonlinear equations with a single unknown parameter $\delta^{(2)}$. If the moveout curve of the PS-wave does not have a minimum on the CMP gather, the objective function includes only the terms with $V_{\mathrm{nmo},P}(p_{P0})$ and $dt/dx|_{x=0}$.

The dip moveout of the PS-wave is represented by either two or just one attribute. To increase the accuracy of the parameter estimation, we can include the whole conventional-spread CMP moveout of the PS-wave into the objective function. In this case, we generate the CMP gather of the PS-wave from equations (4), (4) and (5) for a given value of $\delta^{(2)}$ and find the rms difference between the modeled traveltimes and the "measured" moveout represented by the best-fit shifted hyperbola.

After the parameters of the second layer have been obtained, the parameter-estimation procedure continues downward in a layer-stripping fashion. It should be mentioned that the above operations with the horizontal events are entirely based on the Dix equation and, therefore, do not involve any information about the parameters of the subsurface layers. In contrast, the inversion of the P and PS traveltimes from a dipping reflector cannot be carried out without the parameter-estimation results for the overlying medium. If the overburden is known to be isotropic or elliptically anisotropic, its parameters (V_{P0}, V_{S0}, and $\epsilon = \delta$) can be extracted just from the moveout of horizontal P and PS events. In general VTI media, however, the layer-stripping procedure cannot be performed using horizontal events alone.

Numerical examples

The 2-D inversion algorithm designed for CMP gathers was tested on horizontally layered VTI models with throughgoing dipping interfaces. It was assumed that both horizontal and dipping P and PS events for each layer can be recorded in each layer (Figure 4), so that the input data would include the NMO velocities and vertical traveltimes of both modes from the horizontal reflectors, the NMO velocities and reflection slopes of the dipping P events, and the attributes of the dip moveout of the PS-wave. All these parameters were computed using the exact equations given above and distorted by Gaussian noise to simulate errors in the data. Then the layer-stripping parameter-estimation algorithm based on the objective function (20) was applied to 200 realizations of the noise-contaminated vector of input parameters.

For the three-layer model in Figure 5 the dips do not exceed 35°, and the objective function for the first two layers includes the normalized offset of the traveltime minimum. The scatter in the estimated parameters of the subsurface layer (Figures 5a,b) is the same as in the single-layer inversion results of Paper I. All four pa-

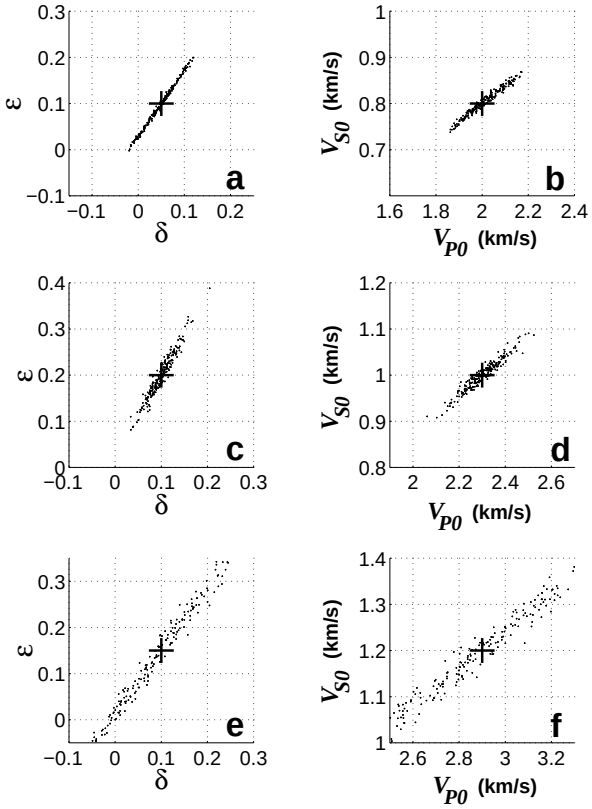

Figure 5. Interval parameters δ, ϵ, V_{P0}, and V_{S0} determined by inverting P and PS moveout data from horizontal and dipping reflectors in a three-layer VTI medium. The layer parameters are the same as in Figure 2; the dips of the interfaces in each layer are (from top to bottom) 30°, 35° and 30°. (a,b) – the results for the top layer (layer 1); (c,d) – layer 2; (e,f) – layer 3; the actual model parameters are marked by the crosses. The input data were distorted by random noise with a standard deviation of 0.5% for the vertical traveltimes, 1.5% for the zero-dip NMO velocities and 2% for the moveout attributes of the dipping events.

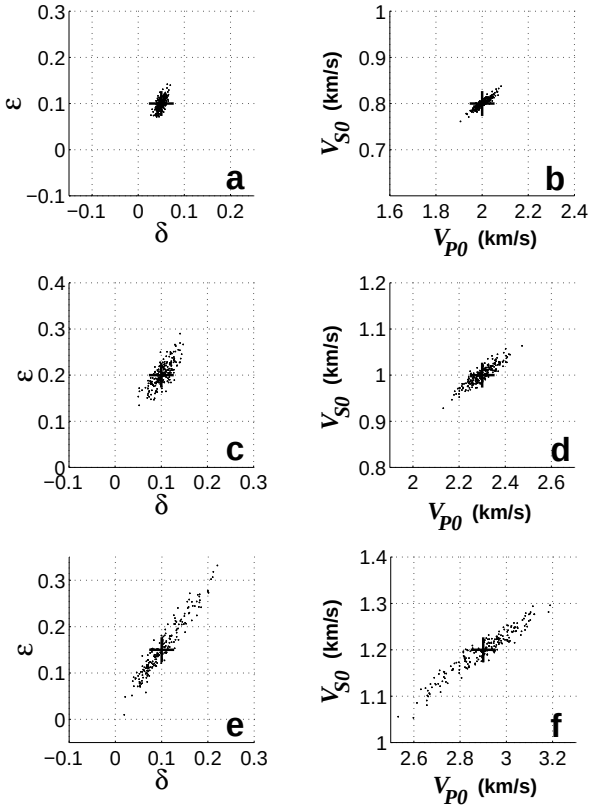

Figure 6. Inversion results for a three-layer VTI medium with steeper dipping interfaces than those in Figure 5 (the dips are 45°, 50° and 55° from top to bottom). The parameters V_{P0}, V_{S0}, ϵ and δ in each layer are the same as in Figures 2 and 5. The layer thicknesses are $z^{(1)} = 0.5$ km, $z^{(2)} = 1.0$ km and $z^{(3)} = 2$ km. (a,b) – the results for layer 1; (c,d) – layer 2; (e,f) – layer 3.

rameters (V_{P0}, V_{S0}, ϵ, δ) are recovered in a reasonably stable fashion, with the quasi-linear trends close to the lines corresponding to the correct values of η (Figure 5a) and V_{P0}/V_{S0} (Figure 5b). This is not surprising because η and V_{P0}/V_{S0} represent the parameter combinations most tightly constrained by the data. The velocity ratio V_{P0}/V_{S0} is determined directly from the vertical traveltimes, while η controls the P-wave NMO velocity from dipping reflectors.

The results for the second layer (Figures 5c,d) are comparable to those for layer 1 because the subsurface layer is relatively thin, and the layer-stripping does not lead to a substantial error amplification. For the bottom layer (Figures 5e,f), however, the scatter in all four parameters becomes noticeably higher due to the distortions in the interval quantities produced by the layer-stripping procedure and error accumulation with depth.

The model in Figure 6 contains a steeper through-going interface, with the dips in the 45–55° range. Comparison of Figures 5 and 6 shows that the the clouds of points become less elongated with increasing dip, which signifies a more stable inversion procedure in all three layers. This result is explained by the higher sensitivity of the P-wave NMO velocity and PS-wave moveout attributes to the anisotropic parameters for larger dips. A similar influence of dip was observed for the single-layer model in Paper I.

Stage 2: CCP gathers

If the reflector has a non-negligible curvature or irregular shape at the scale of the CMP gather, the moveout of converted waves in CMP geometry may be distorted by reflection(conversion)-point dispersal. Since all analytic expressions above, including equation (5), are derived for a plane reflector, the inversion procedure in

this case may produce inaccurate parameter estimates. To mitigate reflection-point dispersal, it is preferable to carry out both velocity analysis and processing of PS-waves on common-conversion-point (CCP) gathers. Resorting PS data into CCP gathers, however, has to be based on a known velocity model. While the lateral position of the reflection (conversion) point in isotropic media is controlled by the V_P/V_S ratio, in VTI media it is also sensitive to the anisotropic coefficients (Rommel, 1997; Thomsen, 1999). Therefore, velocity analysis on CCP gathers in our algorithm is preceded by the move-out inversion in CMP geometry described in the previous section.

Assuming that the inversion on CMP gathers yields a good approximation for the medium parameters, we search for the best-fit interval parameters in a close vicinity of the obtained values. Suppose the parameters of the first (subsurface) layer have been determined, and we can use them to refine the inversion results for the second layer. First, the horizontal PS events from the top and bottom of layer 2 are resorted into CCP gathers using the model determined at the first stage of the inversion. Semblance analysis on these CCP gathers gives updated values of the PS-wave NMO velocities from horizontal reflectors and, therefore, a more accurate estimate of the SV-wave velocity $V^{(2)}_{\mathrm{nmo},SV}(0)$. With the updated $V^{(2)}_{\mathrm{nmo},SV}(0)$ and the previously found values of $V^{(2)}_{\mathrm{nmo},P}(0)$ and $\kappa^{(2)}$, we repeat the computation of the parameters of the second layer for a restricted range of $\delta^{(2)}$.

For each trial set of the medium parameters we reconstruct the dip and depth of the reflector in the second layer and resort the traces with the PS reflection from the dipping interface into CCP gathers. The common conversion point for the dipping PS event is chosen to coincide with the zero-offset reflection point of the dipping P-wave event because reflector dip is determined from the slope of the zero-offset P reflection. Then the PS traveltimes on the CCP gather are generated using equations (4) and (4), and the best-fit $\delta^{(2)}$ is determined from the following objective function:

$$\mathcal{F}_{\mathrm{CCP}} = \left[\frac{V_{\mathrm{nmo},P}(p_{P0}) - V^{\mathrm{meas}}_{\mathrm{nmo},P}(p_{P0})}{V^{\mathrm{meas}}_{\mathrm{nmo},P}(p_{P0})}\right]^2 + t^{\mathrm{rms}}_{PS}, \qquad (21)$$

where t^{rms}_{PS} is the rms difference between the modeled and measured traveltimes of the dipping PS event on the CCP gather.

The general flow of the layer-stripping algorithm remains the same as that for CMP gathers. In principle, it is possible to skip the inversion on CMP gathers altogether and carry out the parameter-estimation for each trial value of δ directly on CCP gathers, but this algorithm is much more time consuming because it involves repeated resorting of PS data.

3-D inversion of wide-azimuth data

The 2-D inversion algorithm requires identifying and inverting P- and PS-waves from two (horizontal and dipping) interfaces for each depth interval, which may be difficult to accomplish in practice. Here we show that it may be possible to obtain all model parameters using a single dipping reflector, if both P and PS data are recorded for a wide range of source-receiver azimuths (the so-called "wide-azimuth" surveys). For simplicity, we restrict ourselves to a homogeneous VTI layer with a dipping lower boundary.

Azimuthally dependent reflection traveltimes of pure modes in anisotropic media were discussed in detail in Grechka and Tsvankin (1998b) and Grechka, Tsvankin and Cohen (1999). NMO velocity can be expressed as the following function of the azimuth α in the horizontal plane (Grechka and Tsvankin, 1998b):

$$V^{-2}_{\mathrm{nmo}}(\alpha) = W_{11}\cos^2\alpha + 2W_{12}\sin\alpha\cos\alpha + W_{22}\sin^2\alpha\,, \qquad (22)$$

where $\mathbf{W}$ is a symmetric matrix defined as $W_{ij} = \tau_0 \frac{\partial p_i}{\partial x_j}$, p_i $(i = 1, 2)$ are the horizontal components of the slowness vector for rays between the zero-offset reflection point and the surface location $\{x_1, x_2\}$ and τ_0 is the one-way traveltime at the CMP location. The derivatives in the expression for W_{ij} are evaluated at the common midpoint. Unless reflection traveltime decreases with offset in at least one azimuthal direction, $V_{\mathrm{nmo}}(\alpha)$ defines an *ellipse* in the horizontal plane.

Since the VTI model is azimuthally isotropic, the axes of the NMO ellipse are parallel to the dip and strike directions of the reflector. For P-waves, both axes and the NMO ellipse as a whole are fully controlled by the parameters $V_{\mathrm{nmo},P}(0)$ and η (Grechka and Tsvankin, 1998b).

The first step of the inversion procedure is to specify a trial value of one of the parameters responsible for P-wave kinematics (e.g., δ) and find the other two (V_{P0} and ϵ) using the parameters $V_{\mathrm{nmo},P}(0)$ and η determined from the P-wave NMO ellipse. Then, similar to the 2-D algorithm, we obtain the horizontal slownesses (ray parameters) p_{1P} and p_{2P} of the zero-offset P-reflection from the reflection slopes on the zero-offset (stacked) section measured in at least two different azimuthal directions (Grechka and Tsvankin, 1998b). For given parameters of the trial model, p_{1P} and p_{2P} can be used to compute the vertical slowness q_P of the zero-offset ray. The slowness vector of the zero-offset ray is orthogonal to the reflector, so it provides both the dip and azimuth of the reflecting interface for the trial model. Reflector azimuth can also be determined from the orientation of the NMO ellipse,

if at least three sufficiently different source-receiver azimuths are available. Next, the zero-offset traveltime of the P-wave can be recomputed into the distance between the CMP and the reflector along the zero-offset ray, thus yielding the reflector depth.

Therefore, given one of the VTI parameters (e.g., δ), wide-azimuth P-wave data are sufficient for obtaining two other parameters (V_{P0} and ϵ) and the spatial position (dip, azimuth and depth) of the reflector. The last step is to estimate δ and the vertical shear-wave velocity V_{S0} (a parameter not constrained by P-wave moveout) using 3-D PS-wave data.

For laterally homogeneous models with a horizontal symmetry plane, common-midpoint reflection moveout of PS-waves is symmetric with respect to zero offset, and their azimuthally dependent NMO velocity represents an ellipse (Grechka, Theophanis and Tsvankin, 1999). Reflector dip, however, makes PS-wave moveout asymmetric for any orientation of the CMP line with respect to the dip plane. Therefore, using an areal (3-D) CMP gather of PS-waves in parameter estimation involves analysis of a traveltime *surface* built as a function of the source and receiver coordinates.

We search for the best-fit pair $\{\delta, V_{S0}\}$ by matching the traveltimes of the PS-wave on a 3-D CMP gather. As in the 2-D problem, it is possible to use the DMO attributes of the PS-wave, such as the moveout slope at zero offset [see equation (11)]. However, we elected to use the whole traveltime surface and defined the objective function as the rms difference between the measured traveltimes and those computed for a trial model using the parametric traveltime-offset relationships (6), (7) and (10). The minimization of the objective function is carried out using the simplex method. Since the forward-modeling operation does not involve multiazimuth and multioffset two-point ray tracing, the algorithm allows for a fast examination of a relatively wide range of both unknown parameters.

The 3-D inversion procedure was tested on ray-traced reflection traveltimes of P- and PS-waves generated for a VTI layer with the parameters listed in the caption of Figure 7. To determine the input PS traveltimes on a regular $[x, y]$ grid of source locations, the traveltime surface was approximated by a 2-D quartic polynomial in the horizontal source coordinates. The times at the grid points were then distorted by Gaussian noise with a standard deviation of 1% (Figure 8). The same polynomial approximation was used for the PS traveltime surfaces computed for each trial model. The inversion algorithm searched for the model providing the smallest rms time residual at the grid points (rather than at the original source locations).

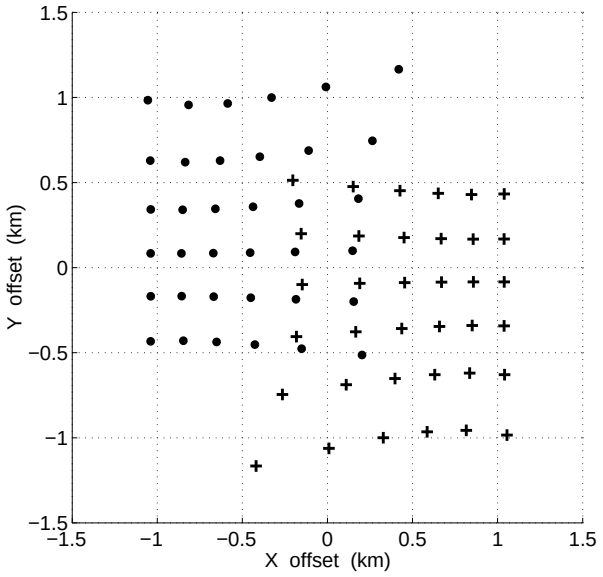

Figure 7. The sources (dots) and receivers (crosses) of the areal (3-D) CMP gather of PS-waves used in the test of the inversion algorithm. The model includes a homogeneous VTI layer with a plane dipping boundary. The VTI parameters are $V_{P0} = 2$ km/s, $V_{S0} = 1$ km/s, $\epsilon = 0.3$, $\delta = 0.1$; the reflector dip is 15°, the azimuth of the dip plane coincides with the x-axis, the depth under the CMP is 1 km.

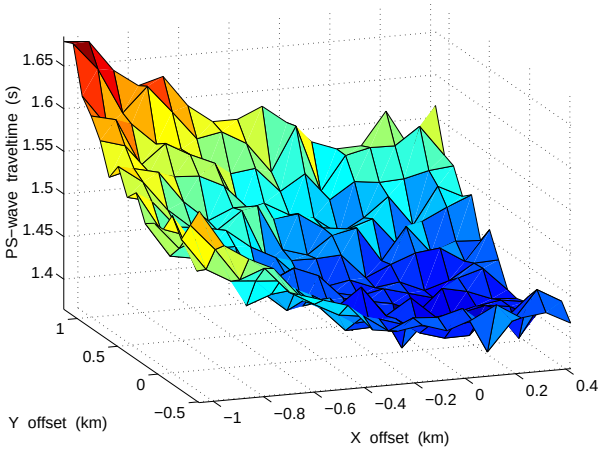

Figure 8. The traveltimes of the reflected PS-wave on the areal CMP gather (plotted as a function of the source coordinate) after the approximation by a 2-D quartic polynomial and addition of Gaussian noise.

The results of the inversion are quite close to the actual values of the VTI parameters: $V_{P0} = 2.02$ km/s (error=0.02 km/s), $V_{S0} = 1.01$ km/s (error=0.01 km/s), $\epsilon = 0.29$ (error=–0.01), $\delta = 0.09$ (error=–0.01). The dip, azimuth and depth of the reflector were also reconstructed with high accuracy. It should be emphasized that the reflector dip in this test was quite mild (15°).

In principle, the model can be refined by resorting the PS data into areal common-conversion-point gathers and repeating the inversion. This procedure is similar to our 2-D algorithm operating with CCP gathers, but resorting PS data in 3-D is much more costly.

Reconstruction of asymmetric PS moveout

The inversion algorithms described above require reconstructing the PS traveltime curve (in 2-D) or surface (in 3-D) from reflection data. Conventional semblance techniques for pure-mode reflections are developed for moveout functions symmetric with respect to zero offset and, therefore, cannot be applied to either CMP or CCP gathers of PS-waves converted at a dipping interface. In Paper I, we suggested to perform semblance analysis of mode conversions along hyperbolas *shifted* with respect to zero offset. This approach, however, is accurate only for mild reflector dips and cannot properly account for nonhyperbolic moveout.

Here we use a more robust approach of Bednar (1997) that does not depend on the functional form of the moveout curve and, as an added benefit, yields moveout slopes needed for the inversion. An estimate of the local slope p of the traveltime curve $t(x)$ can be obtained from the seismograms $u(x,t)$ as (Bednar, 1997)

$$p = \frac{\left\langle \frac{\partial[u]}{\partial x} \frac{\partial[u]}{\partial t} \right\rangle}{\left\langle \frac{\partial[u]}{\partial t} \frac{\partial[u]}{\partial t} \right\rangle}, \tag{23}$$

where $\langle \ldots \rangle$ and $[\ldots]$ denote averaging over t and x, respectively; the derivatives are computed through finite differences.

To illustrate the performance of equation (23), we applied it to synthetic PS-wave seismograms shown in Figures 9a and 10a. The ticks in Figures 9b and 10b show the estimated slopes $p(x,t)$ for which the normalized coherency

$$C = \frac{\left\langle \frac{\partial[u]}{\partial x} \frac{\partial[u]}{\partial t} \right\rangle}{\sqrt{\left\langle \frac{\partial[u]}{\partial x} \frac{\partial[u]}{\partial x} \right\rangle \left\langle \frac{\partial[u]}{\partial t} \frac{\partial[u]}{\partial t} \right\rangle}} \tag{24}$$

is larger than 0.8.

Clearly, the reconstructed slopes closely follow the correct moveout curve (solid line in Figures 9b and 10b) in areas of a relatively strong signal. Even the high level of noise in Figure 10 does not prevent the algorithm based on equation (23) from reconstructing the moveout function for a wide range of offsets. The ticks outside the PS event are associated with the noise that sometimes produces isolated coherency values exceeding the threshold $C = 0.8$. Although this example was generated for a 2-D model, Bednar's (1997) method can be applied in a similar way to traveltime *surfaces* of PS-waves used in 3-D inversion.

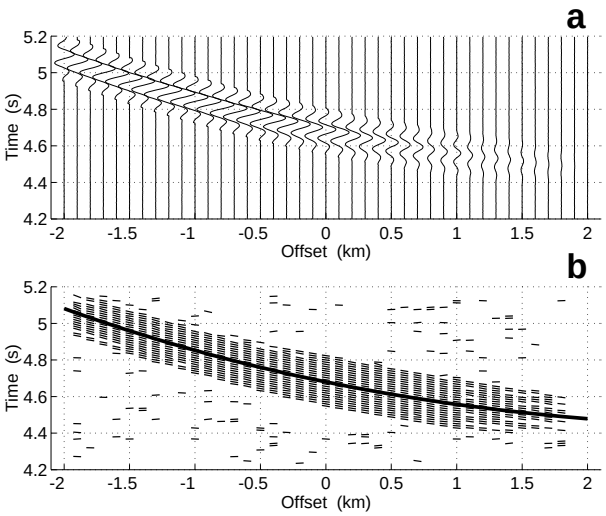

Figure 9. (a) Ray-traced seismogram of the PSV-wave on a CMP gather computed for the model from Figure 2c. The data are contaminated by Gaussian noise with the variance equal to 0.5% of the maximum amplitude. (b) The estimates of local slopes (ticks) and the exact traveltime curve (solid line). The spatial averaging window $[\ldots]$ is 0.2 km (twice the offset increment); the temporal window $\langle \ldots \rangle$ is 8 ms (twice the time increment).

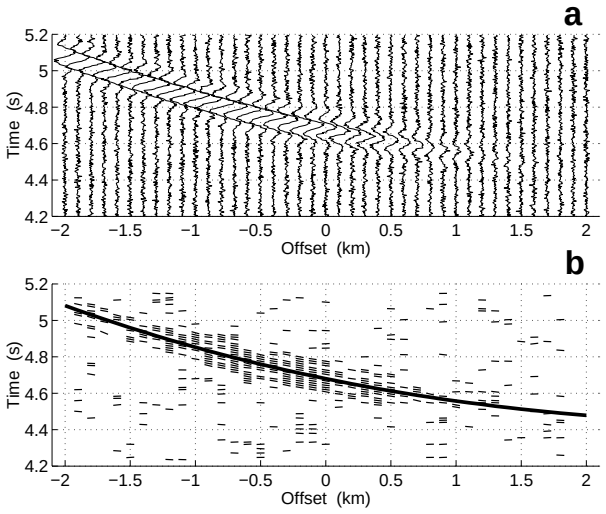

Figure 10. Same as Figure 9, but with the variance of the noise is 10% of the maximum amplitude.

Discussion and conclusions

Most recent applications of converted waves were focused on improved imaging of targets poorly illuminated by P-wave data. In transversely isotropic media, $PS(PSV)$-waves can also play an important role in parameter estimation because they are governed by the same anisotropic coefficients (ϵ and δ) as P-waves. While P-wave reflection data contain enough information to carry out time-domain processing (NMO, DMO and time

migration), they cannot be used to constrain the depth scale in horizontally layered VTI models above a dipping or horizontal reflector. [The recent work of Grechka and Tsvankin (1999) and Le Stunff et al. (1999) indicates that for some piecewise homogeneous VTI media with *dipping* interfaces in the overburden P-wave moveout can be inverted for the vertical velocity.]

In our previous paper on this subject (Tsvankin and Grechka, 1999; Paper I) we developed a general 2-D analytic representation of reflection moveout of mode conversions in symmetry planes of homogeneous anisotropic media and applied it to the joint inversion of reflection traveltimes of P- and PS-waves in a VTI layer. Combination of P and PS moveout data from a horizontal and a dipping reflector proved to be sufficient for estimating all relevant VTI parameters – ϵ, δ, and the vertical velocities V_{P0} and V_{S0}. An important conclusion of Paper I was that without the moveout attributes of the dipping PS event the inversion procedure is unstable and may give inaccurate values of the vertical velocities and reflector depth.

Here, the results of Paper I are extended to more realistic layered arbitrary anisotropic media above a plane dipping reflector. Considering 3-D PS-wave data in both common-midpoint (CMP) and common-conversion-point (CCP) geometry, we express the traveltime and the source-receiver vector in a parametric form through the slowness components of P- and S-legs of the reflected ray. After relating the P and S horizontal slownesses (ray parameters) via Snell's law at the reflector, the CMP traveltime curve can be computed without two-point ray tracing. This formalism also gives a concise description of such moveout attributes of the PS-wave, needed in the inversion procedure, as the slope of the moveout curve at zero offset and the normalized offset of the traveltime minimum. Another general analytic result of this work is a proof that the slope of any CMP moveout curve in arbitrary anisotropic heterogeneous media is determined by the difference between the projections of the ray parameters at the source and receiver locations onto the CMP line.

The parametric representation of PS moveout is then used to invert P and PS data for the anisotropic parameters of VTI media. The 2-D inversion algorithm, which operates with surface moveout data originally collected into CMP gathers in the dip direction of the structure, is designed for horizontally layered VTI media with throughgoing dipping reflectors. [The same model was adopted by Alkhalifah and Tsvankin (1995) in their well-known velocity-analysis method based on P-wave data.] The interval NMO velocities of horizontal P and PS events, determined from the conventional Dix equation, are combined with the interval vertical traveltimes to give three equations for four unknown interval parameters (V_{P0}, V_{S0}, ϵ and δ). For a given interval value of δ, we obtain the interval V_{P0}, V_{S0} and ϵ from the horizontal events and fully reconstruct the trial model in the depth domain using the zero-offset traveltime and reflection slope of the dipping P event. Then we calculate the moveout attributes of the PS-wave and the interval NMO velocity of the dipping P event for the trial model and minimize the misfit (objective) function that contains a single unknown parameter (interval δ). After δ and the other interval parameters have been found, the parameter-estimation procedure continues downward.

Converted-wave data in CMP geometry, however, may be corrupted by reflection-point dispersal on non-planar interfaces. Therefore, we suggest to refine the 2-D inversion results by resorting PS data into common-conversion-point (CCP) gathers and repeating the parameter-estimation procedure. Since the generation of the CCP gathers requires knowledge of the velocity model, it is preceded by the inversion of CMP moveout described above.

For wide-azimuth multicomponent 3-D surveys, additional information is provided by the azimuthal variation of P and PS traveltimes. The P-wave NMO ellipse from a dipping reflector in VTI media can be inverted for the zero-dip NMO velocity $V_{\rm nmo}(0)$ and the anisotropic parameter η. The two remaining VTI parameters (e.g., δ and V_{S0}) are then determined from the traveltime surface of the PS-wave recorded on an areal (3-D) CMP gather. Numerical testing shows that P and PS reflections from a single mildly dipping interface are sufficient to estimate all four VTI parameters and build an accurate depth model.

Our inversion algorithms produce the depth distribution of the four parameters responsible for all signatures of P- and $PS(PSV)$-waves in VTI media. Therefore, the inversion results can be used in prestack and poststack depth migration of P-wave data and processing of PS data for models with a stratified VTI overburden. The main practical difficulty in implementing the joint inversion of P- and PS-waves is to identify in a reliable fashion the pure and converted events reflected from the same interface. Also, the extraction of the asymmetric PS traveltime curves (in 2-D) and surfaces (in 3-D) is a complicated operation that may be hampered by strong spatial amplitude variations and phase reversals of the converted wave. To obtain PS moveout from reflection data, we replaced conventional semblance analysis with a more robust algorithm of Bednar (1997) that also yields the local moveout slope for each source-receiver offset.

The 2-D algorithm remains valid without any modification in the vertical symmetry planes of layered orthorhombic media. The more general 3-D analytic formalism and approach to depth-domain velocity analysis can be used not just for vertical transverse isotropy, but also for lower-symmetry anisotropic models.

Acknowledgments

We are grateful to Leon Thomsen (BP-Amoco) and members of the A(nisotropy)-Team of the Center for Wave Phenomena (CWP) at CSM for helpful suggestions. The support for this work was provided by the members of the Consortium Project on Seismic Inverse Methods for Complex Structures at CWP and by the United States Department of Energy by the United States Department of Energy (award #DE-FG03-98ER14908). I. Tsvankin was also supported by the Shell Faculty Career Initiation Grant.

References

Alkhalifah, T., 1997, Seismic data processing in vertically inhomogeneous TI media: Geophysics, **62**, 662-675.

Alkhalifah, T., Tsvankin, I., Larner, K., and Toldi, J., 1996, Velocity analysis and imaging in transversely isotropic media: Methodology and a case study: The Leading Edge, **15**, no. 5, 371-378.

Alkhalifah, T., and Tsvankin, I., 1995, Velocity analysis for transversely isotropic media: Geophysics, **60**, 1550–1566.

Anderson, J.E., Alkhalifah, T., and Tsvankin, I., 1996, Fowler DMO and time migration for transversely isotropic media: Geophysics, **61**, 835–844.

Bednar, J.B., 1997, Least squares dip and coherency attributes: SEP Report #95, 219–225.

Grechka, V., Theophanis, S., and Tsvankin, I., 1999, Joint inversion of P- and PS-waves in orthorhombic media: Theory and a physical-modeling study: Geophysics, **64**, 146-161.

Grechka, V., Tsvankin, I., and Cohen, J.K., 1999, Generalized Dix equation and analytic treatment of normal-moveout velocity for anisotropic media: Geophys. Prosp., **47**, 117-148.

Grechka, V., and Tsvankin, I., 1998a, Feasibility of non-hyperbolic moveout inversion in transversely isotropic media: Geophysics, **63**, 957-969.

Grechka, V., and Tsvankin, I., 1998b, 3-D description of normal moveout in anisotropic inhomogeneous media: Geophysics, **63**, 1079-1092.

Grechka, V., and Tsvankin, I., 1999, NMO surfaces and Dix-type formulae in heterogeneous anisotropic media: 69th Ann. Internat. Mtg., Soc. Expl. Geophys., Expanded Abstracts, 1612–1615.

Grechka, V., and Tsvankin, I., 2000, Velocity analysis of converted waves based on hyperbolic moveout equation: This volume.

Le Stunff, Y., Grechka, V., and Tsvankin, I., 1999, Depth-domain velocity analysis in VTI media using surface P-wave data: Is it feasible?: this volume.

Rommel, B., 1997, Stacking charts for converted waves in a transversely isotropic medium: Center for Wave Phenomena Research Report (CWP-252).

Seriff, A.J., and Sriram, K.P., 1991, $P-SV$ reflection moveouts for transversely isotropic media with a vertical symmetry axis: Geophysics, **56**, 1271–1274.

Thomsen, L., 1986, Weak elastic anisotropy: Geophysics, **51**, 1954–1966.

Thomsen, L., 1999, Converted-wave reflection seismology over inhomogeneous, anisotropic media: Geophysics, **64**, 678–690.

Tsvankin, I., 1996, P-wave signatures and notation for transversely isotropic media: An overview: Geophysics, **61**, 467–483.

Tsvankin, I., and Grechka, V., 2000, Dip moveout of converted waves and parameter estimation in transversely isotropic media: Geophys. Prosp., **48**, 257–292.

Tsvankin, I., and Thomsen, L., 1994, Nonhyperbolic reflection moveout in anisotropic media: Geophysics, **59**, 1290–1304.

Tsvankin, I., and Thomsen, L., 1995, Inversion of reflection traveltimes for transverse isotropy: Geophysics, **60**, 1095–1107.

APPENDIX A: 3-D traveltime-offset relationships for the PS-wave

Single arbitrary anisotropic layer

Suppose the mode conversion occurs at a plane dipping interface beneath an anisotropic homogeneous layer. Similarly to the 2-D case treated in Paper I, the traveltime along the P-wave leg can be found as

$$t_P = \frac{z_r}{g_P \cos\psi_P} = \frac{z_r}{g_{3P}}, \tag{A1}$$

where $z_r = RD$ is the depth of the reflection point R, ψ_P is the angle between the P-ray and the vertical and g_P is the P-wave group velocity (Figure 3). The vertical component g_3 of the group-velocity vector, expressed through the slowness vector, has the form (Grechka, Tsvankin and Cohen, 1999)

$$\frac{1}{g_3} = q - p_1\, q_{,1} - p_2\, q_{,2}\,, \tag{A2}$$

where p_1 and p_2 are the horizontal components of the slowness vector, $q \equiv p_3$ is the vertical component, $q_{,1} \equiv \partial q/\partial p_1$, and $q_{,2} \equiv \partial q/\partial p_2$. Substituting equation (A2)

into equation (A1) yields the P-wave traveltime as a function of the slowness components:

$$t_P = z_r\,(q_P - p_{1P}\,q_{,1P} - p_{2P}\,q_{,2P})\,, \tag{A3}$$

where $q_{,jP} \equiv \partial q_P/\partial p_{jP}$ $(j = 1, 2)$. Taking into account the contribution of the S-leg, we obtain the following expression for the PS-traveltime:

$$\begin{aligned} t_{PS} &= t_P + t_S \\ &= z_r\,(q_P - p_{1P}\,q_{,1P} - p_{2P}\,q_{,2P} \\ &\quad + q_S - p_{1S}\,q_{,1S} - p_{2S}\,q_{,2S})\,. \end{aligned} \tag{A4}$$

The slowness vectors of the P and S-waves are related to each other by Snell's law at the reflector (i.e., their projections on the reflector should be identical).

The coordinates of the source and receiver can be related to the horizontal component of the group-velocity vector and the length of the ray segment between the reflector and the surface. Assuming that the source (A) excites P-waves and denoting l_P = AR (Figure 3), the horizontal coordinates of the source with respect to the reflection point R are given by

$$x_{iP} = g_{iP}\,\frac{l_P}{g_P} = g_{iP}\,\frac{z_r}{g_P\cos\psi_P} = z_r\,\frac{g_{iP}}{g_{3P}}\;\;(i = 1, 2)\,, \tag{A5}$$

where g_{3P} should be positive because both $l_P > 0$ and $g_P > 0$. For example, if the x_3-axis points upward, the group-velocity vector should correspond to an upgoing wave.

As shown in Grechka, Tsvankin and Cohen (1999), $g_i/g_3 = -q_{,i}$ $(i = 1, 2)$, which allows us to rewrite equation (A5) as

$$x_{iP} = -z_r\,q_{,iP}\;\;(i = 1, 2)\,. \tag{A6}$$

Hence, the source-receiver vector **AC** (Figure 3) is described by

$$\begin{aligned} \mathbf{x}_{PS} &= \mathbf{AC} = \{(x_{1S} - x_{1P}),\,(x_{2S} - x_{2P})\} \\ &= z_r\,\{(q_{,1P} - q_{,1S}),\,(q_{,2P} - q_{,2S})\}\,. \end{aligned} \tag{A7}$$

To find all source-receiver pairs with a common midpoint (CMP) and form a CMP gather, we replace z_r with the vertical distance between the CMP and the reflector ($z_{\rm CMP}$ = OB, Figure A1). First, let us determine the distance BD (see the inset in Figure 3) between the CMP and the projection of the reflection point onto the surface. Since

$$\mathbf{BD} = \frac{1}{2}\,\mathbf{AC} - \mathbf{DC} \tag{A8}$$

and $\mathbf{DC} = -z_r\,\{q_{,1S},\,q_{,2S}\}$, we can use equation (A7) to obtain

$$\mathbf{BD} = \{BD_1, BD_2\} = \frac{z_r}{2}\{(q_{,1P}+q_{,1S}),\,(q_{,2P}+q_{,2S})\}\,. \tag{A9}$$

As illustrated by Figure A1, $z_{\rm CMP}$ can be represented as

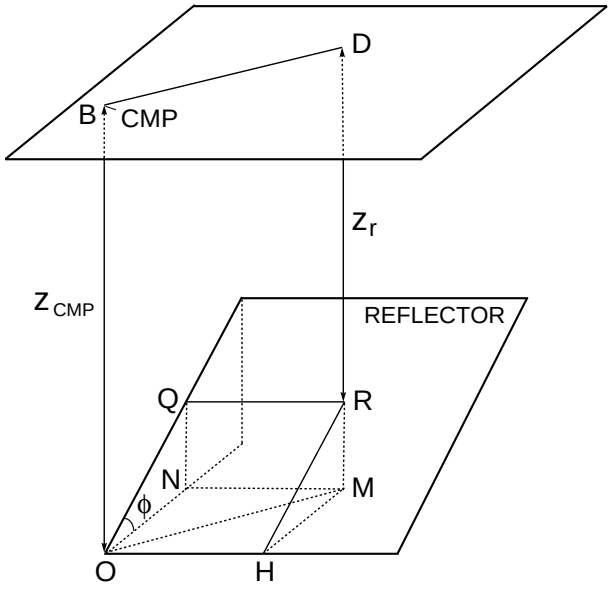

Figure A1. Relationship between the depth z_r = DR of the reflection point R and the vertical distance $z_{\rm CMP}$ = OB between the CMP and the reflector. ON and OH are the dip and strike directions of the reflector (respectively), ϕ is reflector dip. Note that MN⊥ON, OM=BD and $z_{\rm CMP} - z_r$ = RM = QN = ON $\tan\phi$.

$$z_{\rm CMP} = z_r + BD\,\cos(\angle NOM)\,\tan\phi\,, \tag{A10}$$

where ϕ is reflector dip and $\angle NOM$ is the difference between the azimuths of the dip plane and line BD. To ensure the correct sign of $z_{\rm CMP} - z_r$, $\cos(\angle NOM)$ has to be positive if **BD** points in the *updip* direction:

$$\cos(\angle NOM) = \frac{BD_1\,\zeta_1 + BD_2\,\zeta_2}{BD}\,, \tag{A11}$$

where ζ_1, ζ_2 is a horizontal unit vector in the updip direction. Using equation (A9), we find

$$\begin{aligned} &BD\,\cos(\angle NOM) = \\ &\quad \frac{z_r}{2}\,[(q_{,1P} + q_{,1S})\,\zeta_1 + (q_{,2P} + q_{,2S})\,\zeta_2]\,. \end{aligned} \tag{A12}$$

Equations (A10) and (A12) allow us to obtain z_r as a function of $z_{\rm CMP}$:

$$z_r = \frac{z_{\rm CMP}}{1 + \Delta z}\,, \tag{A13}$$

$$\Delta z = \frac{\tan\phi}{2}\,[(q_{,1P} + q_{,1S})\,\zeta_1 + (q_{,2P} + q_{,2S})\,\zeta_2]\,. \tag{A14}$$

Substituting $z_{\rm CMP}$ [equation (A13)] into equation (A4) yields the final expression for the traveltime of the PS-wave:

$$\begin{aligned} t &= \frac{z_{\rm CMP}}{1 + \Delta z}\,(q_P - p_{1P}\,q_{,1P} - p_{2P}\,q_{,2P} \\ &\quad + q_S - p_{1S}\,q_{,1S} - p_{2S}\,q_{,2S})\,, \end{aligned} \tag{A15}$$

where Δz is determined in equation (A14). Similarly, the source-receiver vector (A7) is given by

$$\mathbf{x}_{PS} = \frac{z_{\rm CMP}}{1+\Delta z}\left\{(q_{,1P} - q_{,1S}),\,(q_{,2P} - q_{,2S})\right\}. \qquad \text{(A16)}$$

Layered media

Suppose a plane dipping reflector is now overlaid by a stratified anisotropic medium (all interfaces above the reflector are assumed to be horizontal) with arbitrary symmetry in each layer. As before, the sources and receivers are collected into either CCP gathers corresponding to a fixed conversion point or CMP gathers with different orientation (Figure 3).

To find the traveltime and offset on CCP gathers, it is sufficient to sum up the single-layer solutions from the previous section. Using equation (A4), the traveltime of the wave converted at the N-th interface can be written as

$$\begin{aligned} t_{PS} &= t_P + t_S \\ &= \sum_{\ell=1}^{N} z^{(\ell)}\,(q_P^{(\ell)} - p_{1P}\,q_{,1P}^{(\ell)} - p_{2P}\,q_{,2P}^{(\ell)} \\ &\quad + q_S^{(\ell)} - p_{1S}\,q_{,1S}^{(\ell)} - p_{2S}\,q_{,2S}^{(\ell)}), \end{aligned} \qquad \text{(A17)}$$

where $z^{(\ell)}$ is the thickness of layer ℓ; for layer N, the thickness $z^{(N)}$ should be measured above the reflection (conversion) point. The horizontal components of the slowness vector for both waves (p_{iP} and p_{iS}, $i = 1, 2$) remain constant between the reflector and the surface because the medium along the raypath is horizontally homogeneous.

Likewise, for the source-receiver vector equation (A7) yields

$$\begin{aligned} \mathbf{x}_{PS} &= \{(x_{1S} - x_{1P}),\,(x_{2S} - x_{2P})\} \\ &= \left\{\left[\sum_{\ell=1}^{N} z^{(\ell)}\,(q_{,1P}^{(\ell)} - q_{,1S}^{(\ell)})\right]\right. \\ &\quad \left.\left[\sum_{\ell=1}^{N} z^{(\ell)}\,(q_{,2P}^{(\ell)} - q_{,2S}^{(\ell)})\right]\right\}. \end{aligned} \qquad \text{(A18)}$$

Therefore, after expressing p_{iS} through p_{iP} (or vice versa) using Snell's law at the reflector, CCP gathers in layered media can be generated in a rather straightforward way from equations (A17) and (A18).

Expressions for CCP gathers can be adapted for CMP geometry by replacing $z^{(N)}$ with the thickness of layer N beneath the CMP ($z_{\rm CMP}^{(N)}$). Despite the presence of multiple layers above the reflector, $z_{\rm CMP}^{(N)}$ can be expressed in the form of the single-layer equation (A10):

$$z_{\rm CMP}^{(N)} = z^{(N)} + BD\,\cos(\angle NOM)\,\tan\phi, \qquad \text{(A19)}$$

where BD is the distance between the CMP and the projection of the reflection point onto the (horizontal) surface and $\angle NOM$ is the azimuth of the line **BD** with respect to the dip plane of the reflector (Figure A1).

Using the relationship between **BD** and the source-receiver vector $\mathbf{AC} = \mathbf{x}_{PS}$ [equation (A8), see the inset in Figure 3)] and equation (A18) leads to

$$\begin{aligned} \mathbf{BD} &= \frac{1}{2}\left\{\left[\sum_{\ell=1}^{N} z^{(\ell)}\,(q_{,1P}^{(\ell)} + q_{,1S}^{(\ell)})\right],\right. \\ &\quad \left.\left[\sum_{\ell=1}^{N} z^{(\ell)}\,(q_{,2P}^{(\ell)} + q_{,2S}^{(\ell)})\right]\right\}. \end{aligned} \qquad \text{(A20)}$$

The term $[BD\,\cos(\angle NOM)]$ is the projection of the vector **BD** on the dip direction of the reflector [see equation (A12)]:

$$\begin{aligned} BD\,\cos(\angle NOM) = \frac{1}{2}\left\{\left[\sum_{\ell=1}^{N} z^{(\ell)}\,(q_{,1P}^{(\ell)} + q_{,1S}^{(\ell)})\right]\zeta_1\right. \\ \left. + \left[\sum_{\ell=1}^{N} z^{(\ell)}\,(q_{,2P}^{(\ell)} + q_{,2S}^{(\ell)})\right]\zeta_2\right\}; \end{aligned} \qquad \text{(A21)}$$

as before, ζ_1, ζ_2 is a horizontal unit vector in the updip direction.

Substituting equation (A21) into equation (A19), we find

$$\begin{aligned} z_{\rm CMP}^{(N)} &= z^{(N)} + \frac{\tan\phi}{2}\left\{\left[\sum_{\ell=1}^{N} z^{(\ell)}\,(q_{,1P}^{(\ell)} + q_{,1S}^{(\ell)})\right]\zeta_1\right. \\ &\quad \left. + \left[\sum_{\ell=1}^{N} z^{(\ell)}\,(q_{,2P}^{(\ell)} + q_{,2S}^{(\ell)})\right]\zeta_2\right\}, \end{aligned} \qquad \text{(A22)}$$

which can be treated as a linear equation for $z^{(N)}$ with the solution

$$\begin{aligned} z^{(N)} = \\ \frac{1}{\Phi}\left(z_{\rm CMP}^{(N)} - \frac{\tan\phi}{2}\left\{\left[\sum_{\ell=1}^{N-1} z^{(\ell)}\,(q_{,1P}^{(\ell)} + q_{,1S}^{(\ell)})\right]\zeta_1\right.\right. \\ \left.\left. + \left[\sum_{\ell=1}^{N-1} z^{(\ell)}\,(q_{,2P}^{(\ell)} + q_{,2S}^{(\ell)})\right]\zeta_2\right\}\right), \end{aligned} \qquad \text{(A23)}$$

where

$$\Phi = 1 + \frac{\tan\phi}{2}\left[(q_{,1P}^{(N)} + q_{,1S}^{(N)})\,\zeta_1 + (q_{,2P}^{(N)} + q_{,2S}^{(N)})\,\zeta_2\right].$$

If the model consists of a single layer, the sum $\sum_{\ell=1}^{N-1}$ in the numerator vanishes, and equation (A23) reduces to equation (A13).

Using $z^{(N)}$ from equation (A23) in equations (A17) and (A18) yields the converted-wave traveltime and source-receiver vector in CMP geometry. The location of the CMP gather is defined by the thickness $z_{\rm CMP}^{(N)}$ of layer N beneath the midpoint.

2-D relationships for symmetry planes

3-D equations developed above can be simplified in the special case of a PS-wave recorded in a vertical sym-

metry plane of a layered anisotropic medium. The incidence plane is also assumed to coincide with the dip plane of the reflector, which makes the problem two-dimensional. P-waves propagating in vertical symmetry planes are coupled to only the in-plane polarized shear wave (SV) and, therefore, generate a single mode conversion.

If the dip plane is aligned with the x_1-axis, the projection of the slowness vector on the axis x_2 vanishes, and the traveltime (A17) simplifies to

$$t_{PS} = t_P + t_S = \sum_{\ell=1}^{N} z^{(\ell)} \left(q_P^{(\ell)} - p_{1P}\, q_{,1P}^{(\ell)} + q_S^{(\ell)} - p_{1S}\, q_{,1S}^{(\ell)}\right). \quad \text{(A24)}$$

The source-receiver offset in 2-D geometry can be found from equation (A18) as

$$x_{PS} = x_{1S} - x_{1P} = \sum_{\ell=1}^{N} z^{(\ell)} \left(q_{,1P}^{(\ell)} - q_{,1S}^{(\ell)}\right). \quad \text{(A25)}$$

Equations (A24) and (A25) are sufficient for modeling common-conversion-point gathers.

To obtain a CMP gather, $z^{(\mathrm{N})}$ in equations (A24) and (A25) should be replaced with $z_{\mathrm{CMP}}^{(\mathrm{N})}$. Substituting $\zeta_1 = 1$ and $\zeta_2 = 0$ into the 3-D expression (A23) yields

$$z^{(\mathrm{N})} = \frac{z_{\mathrm{CMP}}^{(\mathrm{N})} - \frac{\tan\phi}{2} \sum_{\ell=1}^{N-1} \left[z^{(\ell)} \left(q_{,1P}^{(\ell)} + q_{,1S}^{(\ell)}\right)\right]}{1 + \frac{\tan\phi}{2} \left(q_{,1P}^{(\mathrm{N})} + q_{,1S}^{(\mathrm{N})}\right)}. \quad \text{(A26)}$$

APPENDIX B: 3-D expression for the slope of reflection moveout

Here we extend the 2-D results of Paper I by obtaining a simple representation of the apparent slowness (slope) of the common-midpoint moveout curve for any reflected event in 3-D geometry. In contrast to Appendix A, the medium above the reflector can be arbitrary heterogeneous, and the reflecting interface is not necessarily plane.

Let us consider a pure or mode-converted reflected wave recorded on a CMP line that makes the angle α with the x_1-axis (Figure B1). If the CMP location and the orientation (azimuth) of the line are fixed, the traveltime depends only on the source-receiver offset x. The slope of the moveout curve at $x = x_0 = SR$ is given by

$$\left.\frac{dt}{dx}\right|_{x_0} = \left.\frac{d(t_1 + t_2)}{dx}\right|_{x_0}, \quad \text{(B1)}$$

where $t_1(x)$ is the traveltime along the ray segment S_1O_1 from the source to the reflector and $t_2(x)$ corresponds to the segment O_1R_1 from the reflector to the receiver (Figure B1). Following the approach of Paper I but performing the analysis in 3-D, we add to and subtract from

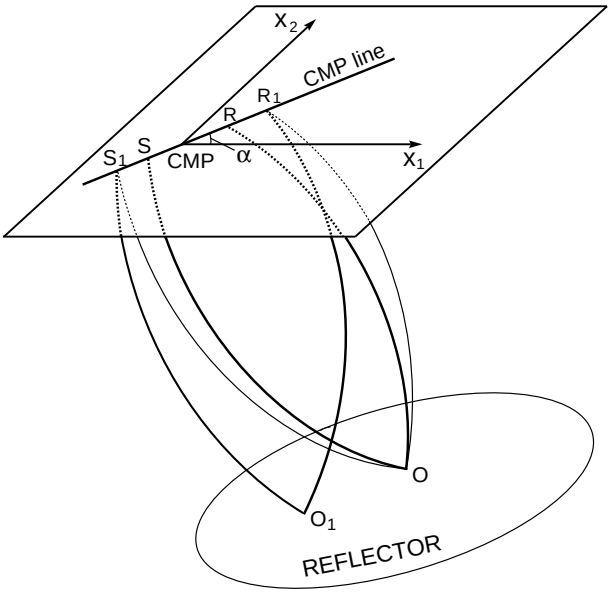

Figure B1. To the derivation of the slope of reflection moveout at the offset $x_0 = SR$. SOR and $S_1O_1R_1$ (bold lines) are the raypaths of the specular CMP reflections at offsets x_0 and $x = S_1R_1$, while S_1OR_1 represents a non-specular reflection. The horizontal coordinates of the reflection points are denoted as $\{\xi_1^{(0)}, \xi_2^{(0)}\}$ (point O) and $\{\xi_1^{(\mathrm{sp})}, \xi_2^{(\mathrm{sp})}\}$ (point O_1).

dt/dx the slope of the *non-specular* traveltime curve t^{ns} computed for raypath S_1OR_1 (i.e., the raypath going through the reflection point corresponding to x_0):

$$\left.\frac{dt}{dx}\right|_{x_0} = \left.\frac{d(t_1^{\mathrm{ns}} + t_2^{\mathrm{ns}})}{dx}\right|_{x_0} + \left.\frac{d(t_1 + t_2 - t_1^{\mathrm{ns}} - t_2^{\mathrm{ns}})}{dx}\right|_{x_0}. \quad \text{(B2)}$$

t_1^{ns} in equation (B2) corresponds to ray segment S_1O, and t_2^{ns} – to OR_1 (Figure B1). The term that involves just the non-specular traveltime can be directly expressed through the slowness vectors of the incident and reflected rays. Indeed, the non-specular raypaths to the source and receiver (S_1O and OR_1) originate at the fixed reflection point O, which implies that the gradient of the traveltime surface for each ray segment is equal to the corresponding slowness vector. Hence,

$$\left.\frac{d(t_1^{\mathrm{ns}} + t_2^{\mathrm{ns}})}{dx}\right|_{x_0} = \left.\frac{d(t_1^{\mathrm{ns}} + t_2^{\mathrm{ns}})}{d(2h)}\right|_{h_0} = \frac{1}{2}\left[p_{\mathrm{R}}(h_0, \alpha) - p_{\mathrm{I}}(-h_0, \alpha)\right], \quad \text{(B3)}$$

where $h \equiv x/2$ is the half offset, $h_0 \equiv x_0/2$, and $p_{\mathrm{I}}(h_0, \alpha)$ and $p_{\mathrm{R}}(h_0, \alpha)$ are the projections of the slowness vectors of the incident ray SO and reflected ray OR (respectively) on the CMP azimuth α; the slowness vectors should be evaluated at the source and receiver locations. To ensure consistency in the signs of the slowness pro-

jections, the positive direction of the CMP line is taken from S to R.

Next, we show that the term that contains the difference between the specular and non-specular traveltimes in equation (B2) goes to zero. Describing the reflecting interface by $\zeta = f(\xi_1, \xi_2)$ (ζ is the vertical coordinate, ξ_1 and ξ_2 are the horizontal coordinates), we can treat the non-specular traveltime $t^{\rm ns}$ for fixed source and receiver positions as a function of the coordinates ξ_1 and ξ_2 of the reflection point. According to Fermat's principle, the specular reflection for a given offset (e.g., the specular ray $S_1O_1R_1$ for the offset x in Figure B1) gives the minimum traveltime (or a saddle of the traveltime surface) for all possible reflected arrivals excited at the same source location and recorded by the same receiver. As a result, the double Taylor series expansion of $t^{\rm ns}(\xi_1, \xi_2)$ at the specular reflection point $\{\xi_1^{(\rm sp)}, \xi_2^{(\rm sp)}\}$ does not contain terms linear in $(\xi_1 - \xi_1^{(\rm sp)})$ and $(\xi_2 - \xi_2^{(\rm sp)})$. Therefore, the non-specular traveltime $t^{\rm ns}(x, \xi_1^{(0)}, \xi_2^{(0)})$ along S_1OR_1 ($\xi_1^{(0)}$ and $\xi_2^{(0)}$ correspond to point O) can be expressed in the following way through the traveltime $t(x) \equiv t(x, \xi_1^{(\rm sp)}, \xi_2^{(\rm sp)})$ computed for the specular ray $S_1O_1R_1$ (Figure B1):

$$t^{\rm ns}(x, \xi_1^{(0)}, \xi_2^{(0)}) = t(x) + \frac{1}{2}\left.\frac{\partial^2 t^{\rm ns}}{\partial \xi_1^2}\right|_{\xi^{(\rm sp)}} (\xi_1^{(0)} - \xi_1^{(\rm sp)})^2 + \left.\frac{\partial^2 t^{\rm ns}}{\partial \xi_1 \, \partial \xi_2}\right|_{\xi^{(\rm sp)}} (\xi_1^{(0)} - \xi_1^{(\rm sp)})\,(\xi_2^{(0)} - \xi_2^{(\rm sp)}) + \frac{1}{2}\left.\frac{\partial^2 t^{\rm ns}}{\partial \xi_2^2}\right|_{\xi^{(\rm sp)}} (\xi_2^{(0)} - \xi_2^{(\rm sp)})^2 + \ldots \,. \tag{B4}$$

Note that the position of the specular reflection point and, therefore, the derivatives of $t^{\rm ns}$ in equation (B4) are functions of the CMP offset x. Using equation (B4) to find the difference between $t^{\rm ns}$ and t and taking the derivative with respect to x leads to

$$\begin{aligned}\frac{d[t^{\rm ns}(x, \xi_1^{(0)}, \xi_2^{(0)}) - t(x)]}{dx} &= \frac{dD_{11}(x)}{dx}\,(\xi_1^{(0)} - \xi_1^{(\rm sp)})^2 \\ &- 2\,D_{11}(x)\,(\xi_1^{(0)} - \xi_1^{(\rm sp)})\,\frac{d\xi_1^{(\rm sp)}}{dx} \\ &+ \frac{dD_{12}(x)}{dx}\,(\xi_1^{(0)} - \xi_1^{(\rm sp)})\,(\xi_2^{(0)} - \xi_2^{(\rm sp)}) \\ &- D_{12}(x)\left[(\xi_1^{(0)} - \xi_1^{(\rm sp)})\,\frac{d\xi_2^{(\rm sp)}}{dx}\right. \\ &\left. + (\xi_2^{(0)} - \xi_2^{(\rm sp)})\,\frac{d\xi_1^{(\rm sp)}}{dx}\right] \\ &+ \frac{dD_{22}(x)}{dx}\,(\xi_2^{(0)} - \xi_2^{(\rm sp)})^2 - 2\,D_{22}(x)\,(\xi_2^{(0)} \\ &- \xi_2^{(\rm sp)})\,\frac{d\xi_2^{(\rm sp)}}{dx},\end{aligned} \tag{B5}$$

where

$$D_{11}(x) \equiv \frac{1}{2}\left.\frac{\partial^2 t^{\rm ns}}{\partial \xi_1^2}\right|_{\xi^{(\rm sp)}}, \tag{B6}$$

$$D_{12}(x) \equiv \left.\frac{\partial^2 t^{\rm ns}}{\partial \xi_1 \, \partial \xi_2}\right|_{\xi^{(\rm sp)}}, \tag{B7}$$

$$D_{22}(x) \equiv \frac{1}{2}\left.\frac{\partial^2 t^{\rm ns}}{\partial \xi_2^2}\right|_{\xi^{(\rm sp)}}. \tag{B8}$$

Since all terms on the right-hand side of equation (B5) vanish at $x = x_0$ ($\xi_1^{(\rm sp)} = \xi_1^{(0)}$, $\xi_2^{(\rm sp)} = \xi_2^{(0)}$),

$$\left.\frac{d[t^{\rm ns}(x, \xi_1^{(0)}, \xi_2^{(0)}) - t(x)]}{dx}\right|_{x_0} = 0\,. \tag{B9}$$

We conclude that the moveout slope can be obtained from the non-specular traveltimes and is equal to one-half of the difference between the projections on the CMP line of the slowness vectors at the source and receiver locations [equation (B3)]:

$$\left.\frac{dt}{dx}\right|_{x_0} = \frac{1}{2}\,[p_{\rm R}(h_0,\,\alpha) - p_{\rm I}(-h_0,\,\alpha)]\,. \tag{B10}$$